Cutoff characteristics of dielectric-filled circular holes embedded in dispersive plasmonic medium

Ki Young Kim

Department of Physics, National Cheng Kung University, 1 University Road, Tainan 70101, China

E-mail: kykim1994@gmail.com

Received May 12, 2009

The cutoff characteristics of dielectric-filled circular holes embedded in a dispersive plasmonic medium are investigated. Since two distinctive operating modes, surface plasmon polariton and circular waveguide modes, can exist in the slow and fast wave regions, respectively, the cutoff characteristics for each are separately investigated for linear and radial polarizations of the guided fields. As a result, the cutoff wavelengths for the linear and radial polarizations with very small subwavelength hole radii are found to be limited by the plasma resonance wavelength and plasma wavelength, which in turn are dependent and independent, respectively, of the dielectric constant of the dielectric filler material.

OCIS codes: 230.7370, 250.5403, 240.6680, 130.2790.

doi: 10.3788/COL20090710.0904.

Since the initial report of Ebbesen's seminal experiment on enhanced optical transmission (EOT) through subwavelength hole arrays in metallic film[1], extensive work has been undertaken to understand this counter-intuitive discovery and identify novel applications for optical and photonic devices based on this phenomenon[2,3]. As a basic element of aperture arrays, various shapes of subwavelength single apertures in metal films have also been intensively studied[3]. The conceptual process of EOT through subwavelength holes in metal films can be qualitatively explained as the coupling of the illumination at the aperture entrance, resulting from an incident plane wave, to the guided modes inside the aperture, and the subsequent decoupling of the electromagnetic energy into a free space mode at the aperture exit on the opposite side with an enhanced intensity compared with that on the input side. Thus, EOT is strongly dependent on the guided modes along the guided structure between the entrance and the exit of the aperture, making precise inspection of the subwavelength guided modes important and indispensible to analyze EOT[4−6]. In addition to their role in EOT, subwavelength guided modes are also crucial in the design of various subwavelength nanoscale waveguiding structures and their diverse derivatives[7,8].

Multi-conductor guiding systems, such as slit or coaxial structures, where the conductors are electrically isolated from each other, do not suffer from a waveguide cutoff due to the existence of transverse electromagnetic (TEM) modes[9−12], enabling the electromagnetic wave to propagate, regardless of the gap dimension between the conductors. However, hollow waveguiding structures embedded in a single conductor, i.e., an electrically non-isolated metal, like circular, elliptical, or rectangular holes in metallic hosts, have finite cutoff wavelengths, even though the cutoff wavelengths are much higher at optical frequencies than those for perfect electric conductor (PEC) structures, as a result of the surface plasmon effect[13−15]. Due to their geometrical simplicity and important applications to scanning near-field optical microscopes, for instance, the fundamental guided modes in subwavelength circular waveguides with plasmonic cladding[16−18] and their radiation characteristics[19] have already been intensively studied at optical frequencies. Plus, the guided dispersions of dielectric-filled circular holes in a plasmonic metal film in relation to the EOT characteristics have recently been investigated for linear polarization[20−22]. Yet, the systematic analysis of the guided mode cutoff characteristics is still insufffcient, especially with regard to the plasmonic dispersion characteristics of a host metallic medium with a wide frequency, even though the cutoff is signiffcant, as it limits the guided propagations along the structure, being the fundamental index of the existence of the guided modes. Accordingly, the cutoff wavelength characteristics of dielectric-filled circular holes in a dispersive plasmonic medium over a wide optical frequency regime are investigated when the hole radius for the linear and radial polarizations of the guided fields is varied. The cutoff wavelengths with very small circular hole dimensions are found to be closely related to the plasma wavelength or plasma resonance wavelength depending on the polarization of the guided field, thereby representing the fundamental limits of the guided mode propagation along subwavelength circular holes in metallic hosts.

A cross-sectional schematic illustration of a dielectric-filled circular hole in a dispersive plasmonic medium is shown in the inset (i) of Fig. 1, where the electromagnetic wave propagation is in the $+z$ direction. The radius of the circular hole is $r = a$ and the hole is filled with a dielectric material with a dielectric constant (relative permittivity) of $\varepsilon_{\rm d} = 1.0$ or $\varepsilon_{\rm d} = 4.0$, each of which is realistic for air or a polymer/semiconductor material at optical frequencies, respectively. The magnetic constants (relative permeability) in both regions are assumed to be unity, i.e., $\mu_{\rm d} = \mu_{\rm p} = 1.0$. The dielectric-filled circular hole is embedded in a dispersive plasmonic medium, the dielectric constant for which is assumed to be a simple lossless Drude model, i.e., $\varepsilon_{\rm p} = 1 - (f_{\rm p}/f)^2$, where f and $f_{\rm p}$ are the operating frequency and plasma frequency, respectively. In this work, $f_{\rm p} = 2175$ THz is assumed to mimic the plasmonic behavior of silver (Ag)[23]. As such,

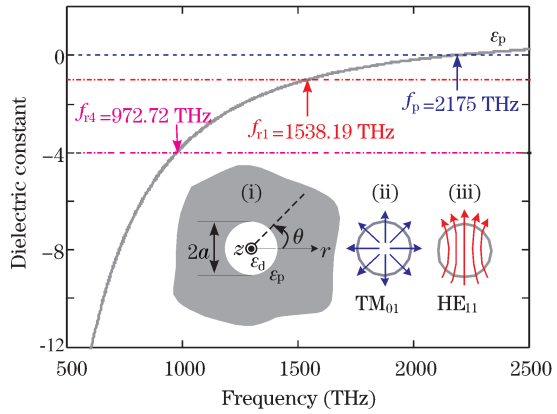

Fig. 1. Dispersion characteristics of Ag-like dispersive plasmonic medium with $\varepsilon_p = 1-(f_p/f)^2$. Inset: (i) cross-sectional schematic view of dielectric-filled circular hole embedded in plasmonic medium; (ii) illustrations of electric field distributions for (ii) TM_{01} and (iii) HE_{11} modes.

the dispersion of the dielectric constant for this Ag-like dispersive plasmonic medium is shown in Fig. 1. Below the plasma frequency, the dispersive dielectric constant becomes negative. Figure 1 also includes another critical frequency, called the plasma resonance frequency, i.e., $f_{ri} = f_p/\sqrt{1+\varepsilon_d}$, where the absolute values of the dielectric constant for the Ag-like medium become the same as those for the dielectric filler materials, which plays an important role in the guided dispersion and cutoff characteristics of this guiding structure. When using this simple Drude model for the Ag-like medium in a wide optical frequency regime, even though the dielectric constant in the higher frequency regime seems to deviate from that for real silver, it can provide a clear picture of the fundamental guiding properties of the guiding structures, which is rather useful in understanding the more important effect of the dispersion of the negative permittivity[10−13]. Furthermore, recent studies have also shown important results for a similar structure and dimensions with a wide optical frequency regime using this simple Drude model for silver[20−22]. Thus, it was decided to use the simple Drude model with a wide optical frequency regime while noting the abovementioned limitation. As a result, a clear picture of the cutoff wavelength characteristics for dielectric-filled circular holes in an Ag-like dispersive plasmonic medium is obtained, which will be discussed shortly.

The negative dielectric constant of the plasmonic medium then facilitates the existence of a surface plasmon polariton (SPP) mode capable of propagating slow waves, i.e., $\beta > k_0\sqrt{\mu_d\varepsilon_d}$, where β and k_0 are the propagation constants of the waveguide and free space, respectively. Meanwhile, in the fast wave region, i.e., $\beta < k_0\sqrt{\mu_d\varepsilon_d}$, there are also guided modes like those usually found in PEC circular waveguides (CWGs). Thus, the existence of the SPP and CWG modes in this structure are mainly attributable to the negative dielectric constant and circular geometry of the hole, respectively, plus these two operating modes are seamlessly connected at the border of $\beta = k_0\sqrt{\mu_d\varepsilon_d}$ to complete a guided mode over the slow and fast wave regions. The characteristic equations for the circular hole embedded in the Ag-like dispersive plasmonic medium can be derived using cylindrical boundary-value problems similar to those for optical fibers[24], the details of which can be given as $P_{CWG/SPP}Q_{CWG/SPP} = R^2$[13], where

$$P_{CWG} = \frac{\varepsilon_d}{k_d}\frac{J'_m(k_d a)}{J_m(k_d a)} + \frac{\varepsilon_p}{k_p}\frac{K'_m(k_p a)}{K_m(k_p a)},$$

$$Q_{CWG} = \frac{\mu_d}{k_d}\frac{J'_m(k_d a)}{J_m(k_d a)} + \frac{\mu_p}{k_p}\frac{K'_m(k_p a)}{K_m(k_p a)},$$

for the CWG mode;

$$P_{SPP} = \frac{\varepsilon_d}{k_d}\frac{I'_m(k_d a)}{I_m(k_d a)} - \frac{\varepsilon_p}{k_p}\frac{K'_m(k_p a)}{K_m(k_p a)},$$

$$Q_{SPP} = \frac{\mu_d}{k_d}\frac{I'_m(k_d a)}{I_m(k_d a)} + \frac{\mu_p}{k_p}\frac{K'_m(k_p a)}{K_m(k_p a)},$$

for the SPP mode, and

$$R = \frac{m\beta}{k_0 a}\left(\frac{1}{k_d^2} + \frac{1}{k_p^2}\right),$$

where k_d and k_p are the propagation constants for the dielectric core and Ag-like dispersive plasmonic cladding regions in the radial direction, respectively, and are given by $k_d = k_0\left(\mu_d\varepsilon_d - \bar{\beta}^2\right)^{1/2}$ and $k_p = k_0\left(\bar{\beta}^2 - \mu_p\varepsilon_p\right)^{1/2}$ for the CWG mode, respectively, and $k_d = k_0\left(\bar{\beta}^2 - \mu_d\varepsilon_d\right)^{1/2}$ and $k_p = k_0\left(\bar{\beta}^2 - \mu_p\varepsilon_p\right)^{1/2}$ for the SPP mode, respectively, where $\bar{\beta}\,(=\beta/k_0)$ is the normalized propagation constant. Plus, $J_m(\cdot)$ and $I_m(\cdot)$ are ordinary and modified Bessel functions of the first kind representing the field behavior inside the hole region for the CWG and SPP modes, respectively, and $K_m(\cdot)$ is a modified Bessel function of the second kind representing the field behavior in the plasmonic medium. Prime denotes the differentiation with respect to r, and m is the azimuthal eigenvalue related to the polarization of the guided fields. If $m = 0$, R also becomes zero, splitting the degenerated characteristic equation into $P_{CWG/SPP} = 0$ or $Q_{CWG/SPP} = 0$, which are the characteristic equations for the transverse magnetic (TM) and transverse electric (TE) modes, respectively, where neither mode has an angular dependence on the electromagnetic field distributions in the guiding cross-section. Among the modes with no angular dependence, the TM_{01} mode, i.e., the first TM mode with $m = 0$, represents the radial polarization of the guided fields illustrated in the inset (ii) of Fig. 1. The TE mode is not of current concern, as it does not support the SPP mode[13]. The HE_{11} mode, which is a TM-like hybrid mode, is referred to as the first mode with $m = 1$, representing the linear polarization of the guided fields, as illustrated in the inset (iii) of Fig. 1. This linearly polarized HE_{11} mode is useful in many practical applications, as it can be easily excited and coupled to the circular guiding structure by conventional end-fire coupling. Meanwhile, the radial polarized TM_{01} mode is known to be capable of possessing a smaller spot size than that of the linearly polarized mode[25], which is important for imaging applications, even though it is more difficult to generate[26]. Therefore, these two polarizations are the main focus of this work, and solutions of the characteristic equations reveal

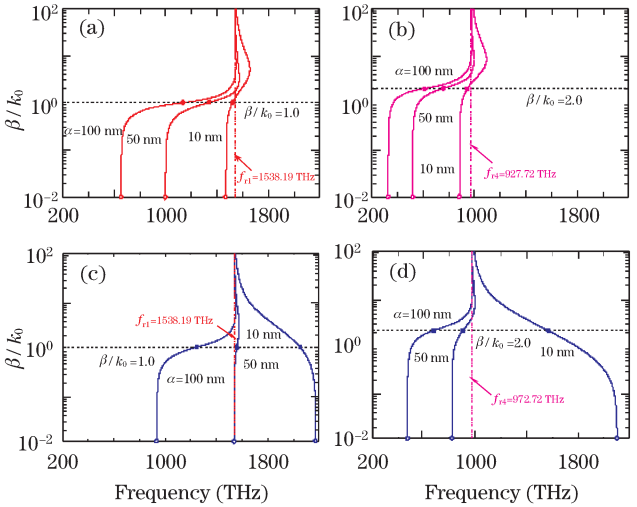

Fig. 2. Guided dispersion characteristics of dielectric-filled circular holes in Ag-like dispersive plasmonic medium for a = 10, 50, and 100 nm. (a) HE_{11} mode for ε_d = 1.0, (b) HE_{11} mode for ε_d = 4.0, (c) TM_{01} mode for ε_d = 1.0, and (d) TM_{01} mode for ε_d = 4.0.

the guided dispersion characteristics of the propagation constants that possess fundamental information, including the cutoff wavelengths.

Figure 2 shows the guided dispersion characteristics of the dielectric-filled circular waveguides embedded in the Ag-like dispersive plasmonic medium over a wide optical frequency regime, where the dielectric constants of the Ag-like medium were $|\varepsilon_p| < \varepsilon_d$ as well as $|\varepsilon_p| > \varepsilon_d$. The vertical dotted and dashed lines represent the plasma resonance frequencies, previously given by $f_{ri} = f_p/\sqrt{1+\varepsilon_d}$, where the subscript i represents the values of the dielectric constants used in this work. The overall guided dispersion curves are found to shift with a change in the plasma resonance frequency. The cutoff for the CWG mode occurs at $\beta/k_0 = 0$ as it exists in the fast wave region, which is normal in the case of a PEC CWG. Similarly, the cutoff for the SPP mode occurs at $\beta/k_0 = \sqrt{\varepsilon_d}$, which is the lowest normalized propagation constant allowed in the slow wave region. Thus, each cutoff for the SPP and CWG modes is marked by solid and open circles, respectively, as shown in Fig. 2. Near the plasma resonance frequency, the guided modes exhibit higher normalized propagation constants, resulting in a lower phase velocity, and backward waves with negative slopes are found to exist above this frequency, where $|\varepsilon_p| < \varepsilon_d$. For the HE_{11} mode, the SPP cutoff frequency is always greater than the CWG cutoff frequency. Whereas the SPP cutoff frequency for the TM_{01} mode is sometimes lower than the CWG cutoff frequency above the plasma resonance frequency, due to the backward wave of the CWG mode, as distinct from the HE_{11} mode. These basic guided dispersion properties are then applied to provide a more detailed understanding of the cutoff wavelength characteristics with wider variations of the hole radius.

Figure 3 shows a comparison of the cutoff wavelength characteristics of the dielectric-filled circular holes in the dispersive plasmonic Ag-like medium for the SPP and CWG modes. The horizontal dashed lines representing a plasma wavelength of λ_p = 137.93 nm, and the dotted

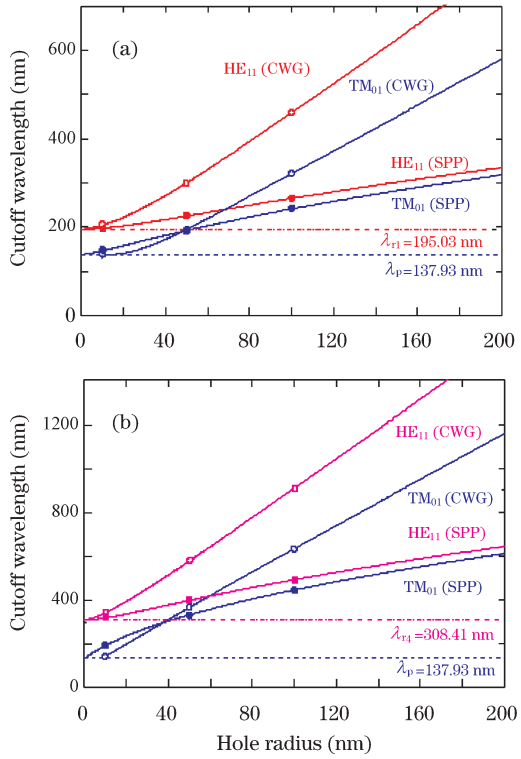

Fig. 3. Cutoff wavelength characteristics of dielectric-filled circular holes in Ag-like dispersive plasmonic medium with respect to hole radius for (a) ε_d = 1.0 and (b) ε_d = 4.0. The dashed lines representing a plasma wavelength of λ_p = 137.93 nm correspond to a plasma frequency of f_p= 2175 THz and the dotted and dashed lines for plasma resonance wavelengths of λ_{r1} = 195.03 nm (for ε_d = 4.0) and λ_{r4} = 308.41 nm (for ε_d = 4.0) correspond to plasma resonance frequencies of f_{r1} = 1538.19 THz and f_{r4} = 972.72 THz, respectively, as shown in Fig. 2. The solid and open circles for the cutoff of the SPP and CWG modes, respectively, in Fig. 2 have been also marked on the curves at a = 10, 50, and 100 nm.

and dashed lines for plasma resonance wavelengths of λ_{r1} = 195.03 nm and λ_{r4} = 308.41 nm correspond to f_p = 2175 THz, f_{r1} = 1538.19 THz, and f_{r4} = 972.72 THz, respectively, as previously shown in Figs. 1 and 2. The solid and open circles for the SPP and CWG mode cutoffs, respectively, in Fig. 2 have been also marked on the curves at a = 10, 50, and 100 nm. As expected, the cutoff wavelengths increase as the hole radius increases. The rate of increase in the cutoff wavelength for the CWG mode is greater than that for the SPP mode for both HE_{11} and TM_{01} modes. Above a plasma resonance wavelength of λ_{ri}, the cutoff wavelength for the CWG mode is longer than that for the SPP modes. Also, the cutoff wavelengths for the TM_{01} mode for the SPP and CWG modes cross near the plasma resonance wavelength. Thus, in the region between the plasma wavelength and the plasma resonance wavelength, the cutoff wavelength for the SPP mode becomes longer than that for the CWG mode due to the backward wave character of the CWG mode, as shown in Fig. 2. When the radius of the hole decreases to a very small subwavelength scale, the cutoff wavelengths for the HE_{11} and TM_{01} modes approach λ_{ri} and λ_p, respectively, representing the minimum cutoff wavelengths for each polarization.

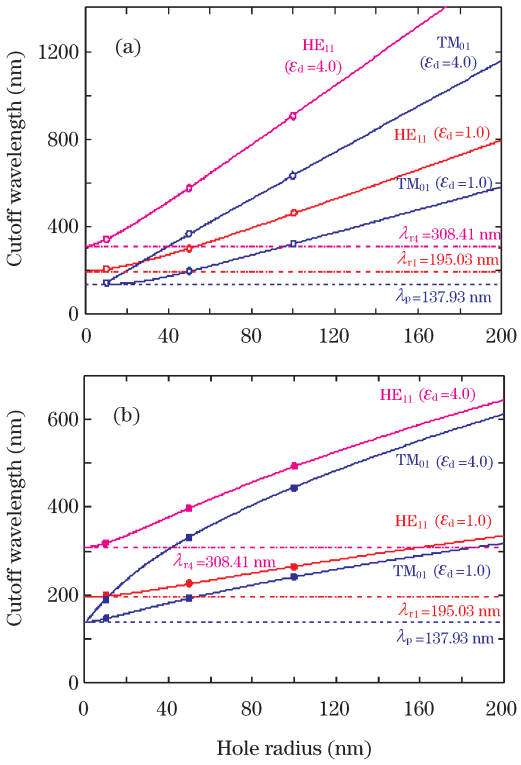

Fig. 4. Cutoff wavelength characteristics of dielectric-filled circular holes in Ag-like dispersive plasmonic medium with respect to hole radius for (a) CWG and (b) SPP modes. The dashed lines representing a plasma wavelength of $\lambda_p = 137.93$ nm correspond to a plasma frequency of $f_p = 2175$ THz and the dotted and dashed lines for plasma resonance wavelengths of $\lambda_{r1} = 195.03$ nm (for $\varepsilon_d = 4.0$) and $\lambda_{r4} = 308.41$ nm (for $\varepsilon_d = 4.0$) correspond to plasma resonance frequencies of $f_{r1} = 1538.19$ THz and $f_{r4} = 972.72$ THz, respectively, as shown in Fig. 2. The solid and open circles for the cutoff of the SPP and CWG modes, respectively, in Fig. 2 have been also marked on the curves at $a = 10$, 50, and 100 nm.

Figure 4 also shows the cutoff wavelength characteristics of the dielectric-filled circular holes in the dispersive plasmonic Ag-like medium, yet provides a clearer view for the influence of the dielectric constant of the dielectric filler material in each operating mode. The cutoff wavelength with a higher dielectric constant is always longer than that with a lower constant due to the higher field concentration in the core region for both CWG and SPP modes, as expected. For the cases of $\varepsilon_d = 1.0$ and $\varepsilon_d = 4.0$, the minimum cutoff wavelengths for the TM_{01} modes are both limited by $\lambda_p = 137.93$ nm, which is independent of the dielectric constant of the dielectric filler material. Meanwhile, with a very small subwavelength hole radius, the HE_{11} modes for the cases of $\varepsilon_d = 1.0$ and $\varepsilon_d = 4.0$ approach plasma resonance wavelengths of $\lambda_{r1} = 195.03$ nm and $\lambda_{r4} = 308.41$ nm, respectively, which are dependent on the dielectric constants of the dielectric filler materials and quite different from the TM_{01} mode case. Finally, it should be noted that the lossless dispersive Drude model for the Ag-like dispersive plasmonic medium is used to characterize the cutoff wavelength characteristics of the dielectric-filled circular holes embedded in the plasmonic medium with respect to variations of the hole radius, even though practical metals at an optical frequency have complex dielectric constants, implying that the current cutoff wavelength characteristics may differ from real situations[16−18,27,28]. Nonetheless, it is believed that this difference can be compensated with the use of an active medium for the core region[29,30]. In this sense, the lossless cutoff wavelength characteristics presented in this work may be signiffcant as fundamental references.

In conclusion, the cutoff wavelength characteristics of dielectric-filled circular holes embedded in a dispersive plasmonic Ag-like medium are investigated with regard to the linear (HE_{11} mode) and radial (TM_{01} mode) polarizations of the guided fields for both CWG and SPP modes. Particularly, in the case of very small subwavelength hole radii, the cutoff wavelengths for the linear and radial polarizations are found to be limited by the plasma resonance wavelength and plasma wavelength, which in turn are dependent and independent, respectively, of the dielectric constant of the dielectric filler material. Due to the absence of the TEM mode, optical and photonic structures and devices based on subwavelength hollow structures, such as the current subwavelength dielectric-filled circular holes embedded in plasmonic metallic hosts, need to be designed carefully to allow proper guided modes along them.

References

1. T. W. Ebbesen, H. J. Lezec, H. F. Ghaemi, T. Thio, and P. A. Wolff, Nature **391,** 667 (1998).
2. F. J. García de Abajo, Rev. Mod. Phys. **79,** 1267 (2007).
3. C. Genet and T. W. Ebessen, Nature **445,** 39 (2007).
4. J. Wuenschell and H. K. Kim, IEEE Trans. Nanotechnol. **7,** 229 (2008).
5. Y. Xie, A. R. Zakharian, J. V. Moloney, and M. Mansuripur, Opt. Express **12,** 6106 (2004).
6. A. R. Zakharian, M. Mansuripur, and J. V. Moloney, Opt. Express **12,** 2631 (2004).
7. S. I. Bozhevolnyi, (ed.) *Plasmonic Nanoguides and Circuits* (World Scientiffc, Singapore, 2009).
8. G. Veronis, Z. Yu, Ş. E. Kocabaş, D. A. B. Miller, M. L. Brongersma, and S. Fan, Chin. Opt. Lett. **7,** 302 (2009).
9. F. I. Baida, A. Belkhir, D. Van Labeke, and O. Lamrous, Phys. Rev. B **74**, 205419 (2006).
10. K. Y. Kim, J. Opt. A: Pure Appl. Opt. **11,** 075003 (2009).
11. K. Y. Kim, "Guided dispersion characteristics of nanoscale plasmonic coaxial lines" J. Comput. Theor. Nanosci. (to be published).
12. K. Y. Kim, Y. K. Cho, H.-S. Tae, and J.-H. Lee, Opt. Express **14,** 320 (2006).
13. K. Y. Kim, Y. K. Cho, H.-S. Tae, and J.-H. Lee, Opto-Electron. Rev. **14,** 233 (2006).
14. R. Gordon and A. Brolo, Opt. Express **13,** 1933 (2005).
15. R. Gordon, L. K. S. Kumar, and A. G. Brolo, IEEE Trans. Nanotechnol. **5,** 291 (2006).
16. L. Novotny and C. Hafner, Phys. Rev. E **50,** 4094 (1994).
17. B. Prade and J. Y. Vinet, J. Lightwave Technol. **12,** 6 (1994).
18. U. Schröter and A. Dereux, Phys. Rev. B **64,** 125420 (2001).
19. T. I. Kuznetsova and V. S. Lebedev, Phys. Rev. E **78,** 016607 (2008).
20. P. B. Catrysse and S. Fan, J. Nanophoton. **2,** 021790

(2008).

21. P. B. Catrysse, H. Shin, and S. Fan, J. Vac. Sci. Technol. B **23,** 2675 (2005).
22. H. Shin, P. B. Catrysse, and S. Fan, Phys. Rev. B **72,** 085436 (2005).
23. M. A. Ordal, L. L. Long, R. J. Bell, S. E. Bell, R. R. Bell, R. W. Alexander, Jr., and C. A. Ward, Appl. Opt. **22,** 1099 (1983).
24. R. E. Collin, *Field Theory of Guided Waves* (2nd edn.) (IEEE Press, New York, 1990).
25. R. Dorn, S. Quabis, and G. Leuchs, Phys. Rev. Lett. **91,** 233901 (2003).
26. T. Hirayama, Y. Kozawa, T. Nakamura, and S. Sato, Opt. Express **14,** 12839 (2006).
27. K. J. Webb and J. Li, Phys. Rev. B **73,** 033401 (2006).
28. J. Olkkonen, K. Kataja, and D. G. Howe, Opt. Express **13,** 6980 (2005).
29. M. P. Nezhad, K. Tetz, and Y. Fainman, Opt. Express **12,** 4072 (2004).
30. S. A. Maier, Opt. Commun. **258,** 295 (2006).